Trabajos de Geología, Universidad de Oviedo, 29 : 157-163 (2009)

Evidence for water-assisted diffusion creep in the mylonitic gneisses of Giuncana, northern Sardinia, Italy

L. CASINI[1]*, P. SENSERINI[2] AND G. OGGIANO[1]

[1]*Istituto di Scienze Geologico-Mineralogiche, Università di Sassari, Italy.*

[2]*Dipartimento di Scienze della Terra, Università di Siena, Italy.*

[*]*e-mail: casini@uniss.it*

Abstract: Quartz ribbons in Variscan, water-rich, amphibolite facies (580-635 ºC; 6.5-7 kbar) mylonitic paragneisses from the Giuncana-Badesi shear zone (GBsz), north Sardinia, Italy, preserve recrystallized grain-size on the millimetre-scale, with lobate/cuspate quartz-feldspar phase boundaries. Feldspars cusps preferentially develop at foliation-perpendicular phase boundaries, strongly aligned with the inferred direction of finite extension. This microstructure is significantly different from the coeval, water-deficient, migmatite mylonites observed along the GBsz around Badesi, where a fine, dynamically recrystallized, quartz-feldspar matrix wraps around sigmoidal feldspar porphyroclasts. This difference indicates that the strain-induced recrystallization mechanism in migmatite mylonites is progressive subgrain-rotation bulging, whereas in paragneiss mylonites the dominant recrystallization mechanism is grain boundary migration coupled with diffusional creep. The volume diffusion localized within quartz ribbons, where feldspars are consumed at quartz-feldspar foliation-parallel boundaries, and growth at quartz-feldspar-quartz foliation-perpendicular boundaries. Both mylonites experienced similar PT conditions during deformation; however the dominant recrystallization mechanism is different. The presence of an H_2O-rich fluids environment in the paragneiss mylonites strongly reflects the switch from dislocation to diffusional creep; hence we suggest that such local fluctuation of water may trigger volume diffusion at unusually low-T.

Keywords: quartz-feldspar mylonites, recrystallization mechanisms, low-T diffusional creep, Sardinia Variscan basement.

The Giuncana-Badesi shear zone (GBsz) is part of the Posada-Asinara Line (PAL), which is one of the main tectonic lineaments crossing the Sardinia Variscan basement (Fig. 1). This tectonic line, originated as a suture zone during N-S collision, in present-day coordinates, between Gondwana and Armorica (Cappelli *et al.*, 1992). After N-S shortening (D1 phase in Carmignani *et al.*, 1994), GBsz was still active during the D2 exhumation phase as dextral shear zone (Carosi *et al.*, 2004). GBsz mylonites experienced extreme deformation during D2 retrograde, top to the SSE shear, in the temperature range between 580-635 °C and 540-520 ºC. Near Badesi, migmatite-mylonites from the Armorica crust have been deformed under relatively water-deficient conditions. The corresponding paragneiss-mylonites from the Gondwana accretionary wedge are exposed few km to the SE, at Giuncana. In the latter, abundance of fluid inclusions

and extensive hydrous retrogression of anhydrous minerals such as kyanite and staurolite indicates a water-rich environment.

The rheological behaviour of quartz/feldspar aggregates depends, essentially, on temperature, strain-rate and water activity (Hirth and Tullis, 1992; Gleason and Tullis, 1995; Stipp *et al.*, 2002). In most amphibolite facies, mylonites deformation results in dislocation creep, and recrystallization processes commonly including bulging, subgrain rotation, and fast grain boundary migration (Hirth and Tullis, 1992; Stipp *et al.*, 2002; Mancktelow and Pennacchioni, 2004), depending on the ease of dislocation climb and boundary diffusion. Rarely, also solution-precipitation processes (Den Brock, 1996; Vernooij *et al.*, 2006b) are predominant. Evidence for strain-induced diffusional creep has been documented in experimentally deformed minerals (Tullis and Yund, 1985; Schmid *et al.*, 1987) and aggregates (Urai, 1983). In naturally deformed rocks, microstructures consistent with strain-induced intra- and inter-crystalline diffusion of material have been exceptionally documented only in high-T gneiss and granulite facies mylonites, where minimum temperature estimates exceed ~700 °C (Behrmann and Mainprice, 1987; Gower and Simpson, 1992; Zulauf *et al.*, 2002).

The microstructure observed in the migmatite-mylonites reflects the dominant recrystallization mechanisms, which are: i) subgrain rotation, and ii) grain boundary migration. This result is consistent with that predicted by theory and observed in most amphibolite facies mylonites (Hirth and Tullis, 1992; Mancktelow and Pennacchioni, 2004). In ribbons from water-rich, paragneiss-mylonites, instead, the quartz-feldspar phase boundaries indicate that recrystallization is partly accommodated by diffusional creep. This difference in microstructures does not reflect significant differences in PT conditions and/or strain-rate, so we suggest that the relative abundance of water in paragneiss-mylonites may trigger volume diffusion at quartz-feldspar contacts.

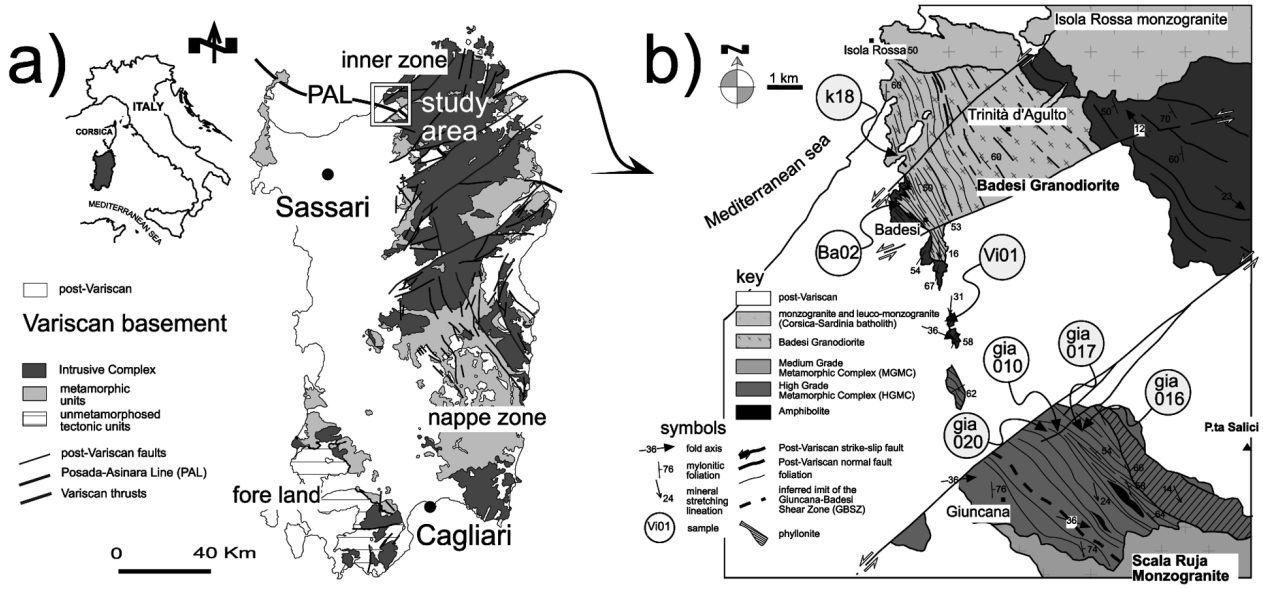

Figure 1. (a) Geological sketch map of Sardinia. Location of figure 1b is shown, (b) simplified structural map of the study area; the position of sampled outcrops is indicated. K18, mylonitic granodiorite; Ba02, Vi01, mylonitic migmatite; Gia020, Gia010, mylonitic paragneiss; Gia016, Gia017, mylonitic quartzite.

Methods

In the study area (Fig. 1), GBsz trends about NW and brings into contact the migmatitic Armorican crust, with the amphibolite facies paragneisses, quartzites and amphibolites of the Gondwana accretionary wedge (Carmignani *et al.*, 1994). The GBsz limits are partly hidden below Permian volcanics and Tertiary marine deposits, but a several hundred meter thick layer of ultra-mylonites marks the shear zone core, indicating a maximum width of 7-8 km. The foliation and mineral fibre lineation (Fig. 1) indicate top to the SSE shear, which is consistent with inferred D2 deformation (Carosi and

Oggiano, 2002). In paragneisses-mylonites, relatively water-rich conditions were assumed to explain: i) the abundance of fluid inclusions, ii) the presence of grain boundary voids, and iii) the extensive hydrous retrogression of staurolite, Al-silicates and biotite. On the other hand, the migmatite-mylonites were deformed under water-deficient conditions. Samples were collected from several outcrops exposed between Badesi and Giuncana, (Fig. 1). Standard and polished thin sections were cut parallel to lineation and perpendicular to foliation, and perpendicular to lineation and foliation (i.e. parallel to XZ and YZ directions of inferred finite strain, respectively), in order to give a 3-D microstructural perspective. In order to compare water-deficient and water-rich mylonites, we collected the gia010 and ba02 samples, both quartz-feldspar mylonites with similar modal proportion between quartz, feldspar and phyllosilicates. Microstructure of quartz-feldspar aggregates was accurately checked on mutually orthogonal sections from both samples. The quartz c- axis preferred orientation has been optically measured by a 5 axis U-Stage on XZ oriented sections, from elongated polycrystalline quartz ribbons.

Migmatite-mylonite (sample Ba02)

These rocks are quartz-feldspar L-S to L-mylonites developed from migmatites of the Armorican crust (Carmignani *et al.*, 1994). In the Badesi area, the original migmatitic layering is strongly transposed parallel to the mylonitic foliation of the adjacent paragneiss-mylonites. An ultramylonite layer, up to 200 m in thickness, developed also parallel to the mylonitic foliation. In the field, alternating millimetre-thick layers of quartz and feldspars, define the foliation, whereas elongated quartz and feldspar grains point out the mineral fibre lineation. The fabric intensity generally increases from the margin of GBsz to the ultramylonite band, where rocks are L-mylonites. The ba02 sample is a banded L>S mylonite collected about 200 m from the ultramylonite layer. Its microstructure results from deformation and grain size reduction of primary quartz, biotite, muscovite, plagioclase and K-keldspar assemblage.

From optical and SEM observation, feldspar-rich layers (Fig. 2) preserve rounded An_{40}-plagioclase and K-feldspar porphyroclasts wrapped by a very fine-grained (<0.005 mm) matrix of recrystallized quartz, An_{22}-plagioclase, and feldspar grains with identical composition to porphyroclasts (SEM-EDS analysis). Quartz-feldspar grains in recrystallized aggregates show a well developed shape preferred orientation (SPO), parallel to the mylonitic foliation. Feldspar porphyroclasts are mantled by aggregates of fine-grained, apparently recrystal-

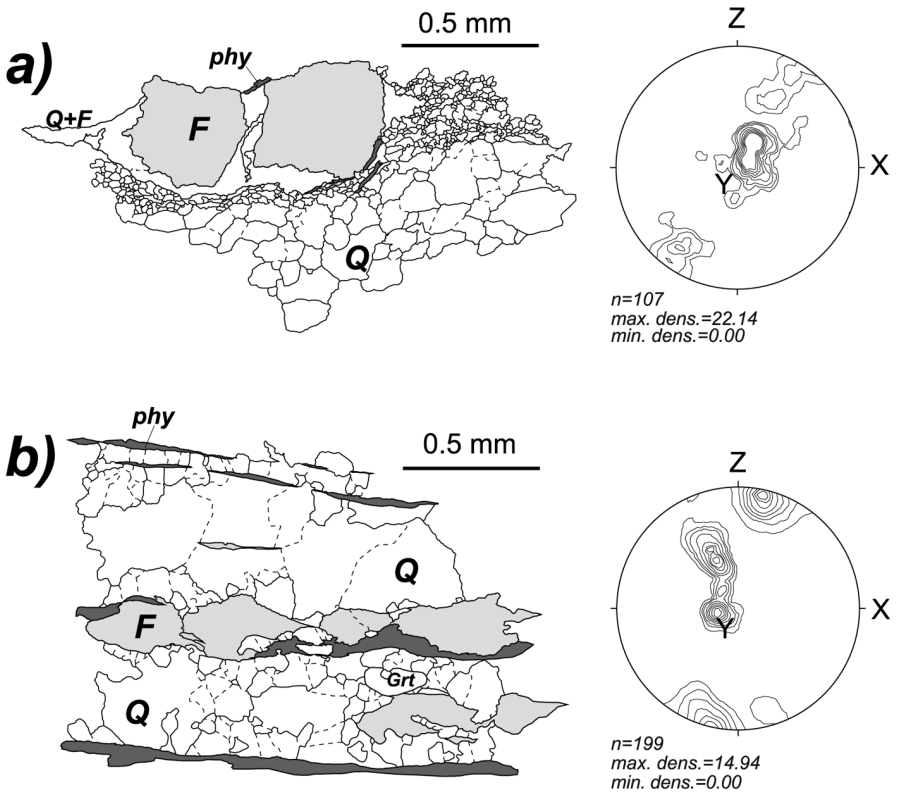

Figure 2. (a) microstructure of samples gia010 and ba02: dotted line, sub-grain boundaries; solid line, high-angle grain boundaries; thick solid line, phase boundaries. Abbreviations: F: K-feldspar and plagioclase; Q: quartz; Grt: garnet; Phy: biotite and muscovite. Scale is indicated, orientation is XZ in each draw, (b) quartz c-axis preferred orientation of ba02 and gia010 ribbons. Equal angle projection, lower hemisphere. Contours intervals shown at 3, 5, 7, 9, 11, 13 multiple of uniform distribution.

lized, K-feldspar and An_{22}-plagioclase crystals. Feldspar cores exhibit some intracrystalline deformation, as indicated by: i) patchy to undulose extinction, ii) rare, optically distinguishable subgrains, and iii) flame perthites.

Quartz layers consist of fine-grained recrystallized aggregates which alternate with larger, monomineralic, ribbons. Recrystallized quartz grains and ribbons show optically visible subgrains and extreme lattice bending, as confirmed by undulose extinction. The boundaries are commonly sutured and/or serrated, but contacts are often diffuse, because of concentration of very fine-grained (<0.005 mm) subgrains and newly formed grains (Fig. 2).

In XZ sections, quartz grains have a strong SPO, about 25° to the mylonitic foliation, whereas in YZ sections the fabric asymmetry is less obvious. Recrystallized fine-grained aggregates show a well developed crystallographic preferred orientation (CPO) around Y, poorly dispersed on the YZ plane (Fig. 2). Distinct bands of similar crystallographic orientation are arranged parallel to ribbons, reflecting a host control by precursor monocrystalline ribbons (Pauli *et al.*, 1996).

Paragneiss mylonite (sample Gia010)

The Giuncana paragneiss mylonite developed from quartz-feldspar metasediments accumulated on the northern Gondwana margin. Layering in these rocks is aligned with the mylonitic foliation, and reflects metamorphic differentiation in domains with variable quartz, feldspar and phyllosilicates content. Approximately, the shape of finite strain range from that of typical S>L to L-S mylonites, with decreasing phyllosilicates content.

The gia010 sample is an L>S mylonite with nearly homogeneous composition. Under the optical microscope, the compositional layering, strong SPO of biotite and muscovite grains, and millimetre-thick, polycrystalline quartz ribbons mark the mylonitic foliation. Feldspar-rich domains (Fig. 2) have effectively a polyphase composition. They consist of $An_{10/24}$-plagioclase and microcline porphyroclasts, generally oblique to foliation, set in aggregates of mixed quartz, garnet, staurolite, tourmaline, muscovite and biotite. Feldspars, as observed in XZ sections, have monoclinic symmetry, consistent with the inferred dextral shear. The internal structure of plagioclase and K-feldspar, however, is free of lattice strains.

Ribbons are characterized by aggregates of dynamically recrystallized quartz grains, with subordinate An_{23}-plagioclase, K-feldspar and biotite grains. Quartz show well developed, perceptible SPO 25° to the mylonitic foliation, and strong, bimodal CPO (Fig. 2). Millimetre-sized quartz grains have their c-axis parallel to the Y direction. These large crystals preserve some rhomb- and prism-parallel subgrains boundaries, but seldom they appear optically free of lattice strains. C-axis of relatively small, recrystallized grains, cluster around the inferred direction of minimum shortening. The quartz-quartz contacts are strongly lobate and sutured, with several indentation microstructures (Jessel, 1987). Nucleation of recrystallized grains and, locally, bulges of one grain into adjacent crystals are common along quartz-quartz contacts.

Strongly elongate feldspars (aspect-ratio up to 20:1) are arranged parallel to the mylonitic foliation, and often show a pinch-and-swell structure. The feldspar boundaries are commonly lobate or gently curved. At quartz-feldspar-quartz triple contacts, feldspar show elongate cusps that point into adjacent quartz domains. Tight cusps preferentially developed at foliation-perpendicular boundaries (Fig. 3), noticeably aligned with the inferred X tectonic direction. At foliation-parallel boundaries, instead, cusps are poorly developed in otherwise gently curved boundaries.

Deformation and PT estimates

PT estimates for the mylonitic deformation (D2) have been calculated from sample gia010, a garnet-biotite gneiss, by the SEM-EDS technique. Operating conditions were 20 Kv acceleration potential, 60 A of current intensity, and 150 nm spot. Natural minerals were utilized as standard, analysis have been corrected to standards taking into account the effect of actual sample parameters such as atomic number (Z), absorption (A) and fluorescence (F), following the ZAF procedure. Closure temperatures for the Fe-Mg exchange between garnet-biotite, garnet-phengite and biotite-phengite pairs were determined from the software thermobarometry v.2.1 (Spear *et al.*, 1999).

In feldspar-rich domains, garnet is present in two distinct microstructural sites. In site 1, garnets are small, idiomorphic grains trapped within oligoclase porphyroclasts, whereas in site 2 they form large, subhedral porphyroblasts in microtextural equilibrium with the foliation. The garnet-rim, biotite and phengite compositions were determined in both domains. Results

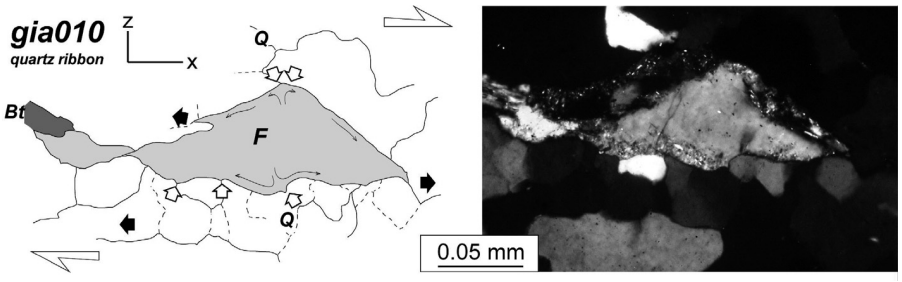

Figure 3. Model for quartz-feldspar phase boundary mobility and photomicrograph of the same microstructure: F: potash feldspar; Bt: biotite (all other crystals are quartz); dark arrows: growing cusp; white arrows: consuming cusp. Thin arrows indicated the inferred pathways of volume diffusion along quartz-feldspar boundaries. The scale and orientation of the thin section is indicated.

from site 2 are consistent with the main mylonitic deformation, whereas compositions of mineral pairs in site 1 give a maximum estimates for the peak temperature (Wu *et al.*, 2002).

Following several calibrations for the garnet-biotite geothermometer (Ferry and Spears, 1978; Hodges and Spears, 1982; Ganguly and Saxena, 1984), the peak temperature was estimated in the range 580-635 °C for site 1. The Fe-Mg exchange between adjacent garnet and phengite (Green and Hellmann, 1982; Hynes and Forest, 1988) is in agreement this result, indicating a temperature range between 580-600 °C. A maximum pressure of 6.5-7 kbar was estimated in site 1, based on the Si-content of phengite in the presence of K-feldspar, flogopite and quartz (Massone and Schreyer, 1987). In site 2, instead, mineral compositions indicate a general retrogression of the conditions at microtextural equilibrium, with temperature range between 520-540 °C, and maximum pressure ~3.5-4 kbar.

Discussion

The microstructure of ba02 is similar to typical amphibolite facies mylonites (Stipp *et al.*, 2002; Mancktelow and Pennacchioni, 2004). The strong CPO of quartz grains within nearly monomineralic ribbons suggests a deformation mechanism dominated by intracrystalline dislocation creep, without significant grain boundary sliding. Quartz c-axis form a monoclinic single girdle, roughly perpendicular to the stretching lineation and tilted 25° apart from the Z axis, whose asymmetry is consistent with the general sense of shear along the GBsz (Schmid and Casey, 1986; Law *et al.*, 1990). The clustering of quartz c-axis around the Y direction results from dislocation glide mainly on the prism <a> and rhomb ± slip systems (Lister and Dornsiepen, 1982). Light maxima appear on the XZ plane, indicating a contribution from basal <a> glide. Crystals suitably oriented for basal <a> slip preferentially localized along incoming micro-shear zone crossing the ribbons, so we suggest that basal <a> glide activated during the late stage of deformation, with decreasing temperature from ~635 °C to ~520 °C. The absence of quartz c-axis around the direction of finite extension indicates that prism-c glide system was not effective, consistently with inferred dry conditions (Mainprice *et al.*, 1986; Okudaira *et al.*, 1995).

Dynamic recrystallization is extensive on ba02 ribbons; however mantled feldspar porphyroclasts show a transitional zone between core and mantle, reflecting progressive subgrain rotation (Guillope and Poirier, 1979). This process is possibly coupled with dismembering of host crystals and subsequent rotation during grain-size reduction, as indicated by some brittle-ductile precursor shear zones (Passchier, 1985; Mancktelow and Pennacchioni, 2004), indicating that the main effect of deformation on this rock is grain size reduction of primary crystals.

The quartz microstructure from gia010 reflects a combination of grain boundary migration, bulging and subgrain rotation recrystallization (Jessel, 1987; Hirth and Tullis, 1992; Stipp *et al.*, 2002), as observed in ba02. Quartz CPO from gia010 ribbons is well developed and closely matches that observed in corresponding domains from migmatite-mylonites (Fig. 2). Also in these rocks, hence, the quartz network deformed through dislocation creep. The microstructure of feldspar grains, instead, is completely different from that observed in ba02 porphyroclasts. Feldspars are apparently strain-free, except for pinch and swell structure, reflecting incipient boudinage on the XY plane.

Also, the strong alignments of feldspar cusps parallel to the X tectonic axis suggest a syntectonic origin for

the boundaries. Two mechanisms might account for deformation of feldspar. The first, that feldspars were deformed by dislocation creep above 500 ºC (Vidal *et al.*, 1980; Olsen and Kohlstedt, 1985) and then completely recovered, is untenable because post-tectonic annealing should have produced randomly oriented cusps (Spry, 1969; Kingery *et al.*, 1976). Also, quartz has faster recovery rates than feldspar at the same temperature, so post-tectonic annealing should have preferentially recovered quartz grains, which is not the case. The latter mechanism requires change of shape without significant lattice strains, and is consistent with HT-diffusion creep (Behrmann and Mainprice, 1987; Gower and Simpson, 1992; Zulauf *et al.*, 2002). The mechanism for syntectonic phase boundary migration may result from preferential feldspar dissolution at foliation-parallel boundaries, migration of material on the grain scale, and precipitation at foliation-perpendicular boundaries (Gower and Simpson, 1992). Following on from this model, smooth cusps, rarely preserved along foliation-parallel boundaries, may represent transient structures reflecting fine scale textural disequilibrium (Fig. 3).

Conclusions

Experiments and natural observations indicate that the rheological behaviour of quartz-feldspar aggregates depends, primarily, on temperature, strain-rate and water activity (Hirth and Tullis, 1992; Gleason and Tullis, 1995; Stipp *et al.*, 2002; Mancktelow and Pennacchioni, 2004). In ba02 migmatite-mylonites, quartz-feldspar microstructure reflects, primarily, dislocation creep and grain size reduction, consistent with typical amphibolite facies mylonites (Passchier, 1985; Law *et al.*, 1990; Stipp *et al.*, 2002; Mancktelow and Pennacchioni, 2004). In the corresponding gia010 paragneiss sample, instead, microstructure reflects textural coarsening, and quartz-feldspar phase boundaries results from a deformation mechanism similar to the boundary-diffusion controlled creep (Coble, 1963). Diffusion creep in quartz-feldspar aggregates is usually reported to occur above ~700-750 ºC (Behrmann and Mainprice, 1987; Gower and Simpson, 1992; Zulauf *et al.*, 2002), or in partially molten aggregates (Dell'Angelo and Tullis, 1988). PT estimates for GBsz mylonites, instead, are consistent with the typical range of temperature at which dislocation creep might occur, hence some factors apart from temperature may enhanced the mobility of material in and along grain boundaries. The localization of diffusion creep only in 'wet' gia010 paragneiss-mylonites, but not in the migmatite-mylonites suggests that water activity is critical for the switch between dislocation- and diffusion creep in the range 580-635 °C. The influence of water possibly reflects the ease of quartz precipitation and dissolution at specific crystallographic orientation (Den Brock, 1996; Vernooij *et al.*, 2006a), triggering volume diffusion in and along the quartz-feldspar contacts. As observed in other amphibolite facies mylonites (Mancktelow and Pennacchioni, 2004), water has, apparently, poor effect on the activity of slip systems in quartz, however it may enhance feldspar ductility, modifying the rheology of quartz-feldspar rocks.

References

Behrmann, J. H. and Mainprice, D. (1987): Deformation mechanisms in a high temperature quartz-feldspar mylonite: evidence for superplastic flow in the lower crust. *Tectonophysics*, 140: 297-305.

Cappelli, B., Carmignani, L., Castorina, F., Di Pisa, A., Oggiano, G. and Petrini, R. (1992): A Hercynian suture zone in Sardinia: geological and geochemical evidence. *Geodin. Acta*, 5, 1-2: 101-118.

Carmignani, L., Carosi, R., Di Pisa, A., Gattiglio, M., Musumeci, G., Oggiano, G. and Pertusati P. C. (1994): The Hercynian chain in Sardinia (Italy). *Geodin. Acta*, 7, 1: 31-47.

Carosi, R., Di Pisa, A., Iacopini, D., Montomoli, C. and Oggiano, G. (2004): The structural evolution of the Asinara Island (NW Sardinia, Italy). *Geodin. Acta*, 17, 5: 309-329.

Carosi, R. and Oggiano, G. (2002): Transpressional deformation in NW Sardinia (Italy): insights on the tectonic evolution of the Variscan belt. *C. R. Geosci.*, 334: 287-294.

Coble, R. L. (1963): A model for boundary-diffusion controlled creep in polycrystalline materials. *J. Appl. Phys.*, 34: 1679-1682.

Dell'Angelo, L. N. and Tullis, J. A. (1988): Experimental deformation of partially melted granitic aggregates. *J. Metamorph. Geol.*, 6: 495-515.

den Brok, B. (1996): The effect of crystallographic orientation on pressure solution in quartzite. *J. Struct. Geol.*, 18: 859-860.

Ferry, J. M. and Spear, F. S. (1978): Experimental calibration of the partitioning of Fe and Mg between biotite and garnet. *Contrib. Mineral. Petr.*, 66: 1100-1106.

Ganguly, J. and Saxena, S. K. (1984): Mixing properties of aluminosilicate garnets: constraints from natural and experimental data, and applications to geothermo-barometry. *Am. Mineral.*, 69: 88–97.

Gleason, G. C. and Tullis, J. (1995): A flow law for dislocation creep of quartz aggregates determined with the molten salt cell. *Tectonophysics*, 247: 1-23.

GOWER, R. J. W. and SIMPSON, C. (1992): Phase boundary mobility in naturally deformed, high-grade quartzfeldspathic rocks: evidence for diffusional creep. *J. Struct. Geol.*, 14: 301-313.

GREEN, T. H. and HELLMANN, P. L. (1982): Fe-Mg partitioning between coexisting garnet and phengite at high pressure and comments on a garnet-phengite geothermometer. *Lithos*, 15: 253-266.

GUILLOPE, M. and POIRIER, J. P. (1979): Dynamic recrystallization during creep of single crystalline halite: an experimental study. *J. Geophys. Res.*, 84: 5557-5567.

HIRTH, G. and TULLIS, J. (1992): Dislocation creep regimes in quartz aggregates. *J. Struct. Geol.*, 14: 145-159.

HODGES, K. V. and SPEAR, F. S. (1982): Geothermometry, geobarometry and the Al_2SiO_5 triple point at Mt. Moosilauke, New Hampshire. *Am. Mineral.*, 67: 1118-1134.

HYNES, A. and FOREST, R.C. (1988): Emperical garnet-muscovite geothermometry in low grade metapelites, Selwyn Range (Canadian Rockies), *J. Metamorph. Geol.*, 6: 297–309.

JESSEL, M. W. (1987): Grain-boundary migration microstructures in a naturally deformed quartzite. *J. Struct. Geol.*, 9: 1007-1014.

KINGERY, W. D., BOWEN, H. K. and UHLMANN, D. R. (1976): *Introduction to Ceramics*. John Wiley & Sons Inc., New York, 1032 pp.

LAW, R. D., SCHMID, S. M. and WHEELER, J. (1990): Simple shear deformation and quartz crystallographic fabrics: a possible natural example from the Torridon area of NW Scotland. *J. Struct. Geol.*, 12: 29-45.

LISTER, G. S. and DORNSIEPEN, U. L. (1982): Fabric transitions in the Saxony granulite terrane. *J. Struct. Geol.*, 4: 81-92.

MAINPRICE, D., BOUCHEZ, J. L., BLUMENFELD, P. and TUBIA, J. M. (1986): Dominant c-slip in naturally deformed quartz: implications for dramatic plastic softening at high temperature. *Geology*, 14: 819-822.

MANCKTELOW, N. S. and PENNACCHIONI, G. (2004): The influence of grain boundary fluids on the microstructure of quartz-feldspar mylonites. *J. Struct. Geol.*, 26: 47-69.

MASSONE, H. J. and SCHREYER, W. (1987): Phengite geobarometry based on the limiting assemblage with K-feldspar, phlogopite, and quartz. *Contrib. Mineral. Petrol.*, 96: 212-224.

OKUDAIRA, T., TAKESHITA, T., IKUO HARA and JUN-ICHI, A. (1995): A new estimate of the conditions for transition from basal <a> to prism [c] slip in naturally deformed quartz. *Tectonophysics*, 250: 31-46.

OLSEN, T. S. and KOHLSTEDT, D. L. (1985): Natural deformation and recrystallization of some intermediate plagioclase feldspars. *Tectonophysics*, 111: 107-131.

PASSCHIER, C. W. (1985): Water-deficient mylonite zones: an example from the Pyrenees. *Lithos*, 18: 115-127.

PAULI, C., SCHMID, S. M., PANOZZO, R. and HEILBRONNER, R. (1996): Fabric domains in quartz-mylonites: localized three-dimensional analysis of microstructure and texture. *J. Struct. Geol.*, 18: 1183-1203.

SCHMID, S. M. and CASEY, M. (1986): Complete fabric analysis of some commonly observed quartz C-axis patterns. *Am. Geophys. Union Monogr.*, 36: 263-286.

SCHMID, S. M., PANOZZO, R. and BAUER, S. (1987): Simple shear experiments on calcite rocks: rheology and microfabric. *J. Struct. Geol.*, 9: 747-778.

SPEAR, F. S., KOHN, M. J. and CHENEY, J. T. (1999): P-T paths from anatectic pelites. *Contrib. Mineral. Petrol.*, 134: 17-32.

SPRY, A. (1969): *Metamorphic Textures*. Pergamon Press, Oxford, 336 pp.

STIPP, M., STÜNITZ, H., HEILBRONNER, R. and SCHMID, S. M. (2002): The eastern Tonale fault zone: a 'natural laboratory' for crystal plastic deformation of quartz over a temperature range from 250 to 750 °C. *J. Struct. Geol.*, 24: 1861-1884.

TULLIS, J. A. and YUND, R. A. (1985): Dynamic recrystallization in feldspar: a mechanism for ductile shear zone formation. *Geology*, 13: 238-241.

URAI, J. L. (1983): Water-assisted dynamic recrystallization and weakening in polycrystalline bischofite. *Tectonophysics*, 96: 125-127.

VERNOOIJ, M. G. C., DEN BROCK, B. and KUNZE, K. (2006a): Development of crystallographic preferred orientations by nucleation and growth of new grains in experimentally deformed quartz single crystals. *Tectonophysics*, 427: 35-53.

VERNOOIJ, M. G. C., KUNZE, K. and DEN BROK, B. (2006b): 'Brittle' shear zones in experimentally deformed quartz single crystals. *J. Struct. Geol.*, 28: 1292-1306.

VIDAL, J. L., KUBIN, L., DEBAT, P. and SOULA, J. C. (1980): Deformation and dynamic recrystallization of Kfeldspar augen in orthogneiss from Montagne Noire, Occitania, southern France. *Lithos.*, 13: 247-255.

WU, C. M., WANG, X. S., YANG, C. H., GENG, Y. S. and LIU, F. L. (2002): Empirical garnet-muscovite geothermometry in metapelites. *Lithos.*, 62: 1-13.

ZULAUF, G., DORR, W., FIALA, J., KOTKOVA, J., MALUSKI, H. and VALVERDE-VAQUERO, P. (2002): Evidence for high-temperature diffusional creep preserved by rapid cooling of lower crust (North Bohemian shear zone, Czech Republic). *Terra Nova*, 14: 343-354.